

# Enhancing the Nonlinear Mutual Dependencies in Transformers with Mutual Information

Anonymous ACL submission

## Abstract

The predictive uncertainty problem exists in Transformers. We present that pre-trained Transformers can be further regularized by employing mutual information to alleviate such issues in neural machine translation (NMT). In this paper, to enhance the representation, we explicitly capture the nonlinear mutual dependencies existing in two types of attention in the decoder to reduce the model uncertainty. Specifically, we employ mutual information to measure the nonlinear mutual dependencies of token-token interactions during attention calculation. Moreover, we resort to InfoNCE for mutual information estimation to avoid the intractable problem. By maximizing the mutual information among tokens, we capture more knowledge concerning token-token interactions from the training corpus to reduce the model uncertainty. Experimental results on WMT'14 En→De and WMT'14 En→Fr demonstrate the consistent effectiveness and evident improvements of our model over the strong baselines. Quantifying the model uncertainty again verifies our hypothesis. The proposed plug-and-play approach can be easily incorporated and deployed into pre-trained Transformer models. Code will be released soon<sup>1</sup>.

## 1 Introduction

Predictive uncertainty ubiquitously exists in deep learning or machine learning based models (Ott et al., 2018a; Xiao and Wang, 2019; Wang et al., 2019; Abdar et al., 2020; Xiao and Wang, 2021). It consists of data uncertainty (aleatoric uncertainty) and model uncertainty (epistemic uncertainty). Data uncertainty mainly results from the noise during the data collection. In practice, model uncertainty depicts whether the model can best describe the data distribution, and model uncertainty significantly attributes to the poor fitting of the data distribution (Wang et al., 2019). Model uncertainty

<sup>1</sup>Anonymous: <https://github.com/self-attention-MI/UE>

	Token-token interactions	Uncertainty	
		Token	Token-token
Transformer	linear	↑	↓ (implicitly)
Our model	linear + nonlinear	↑	↓ (explicitly)

Table 1: Comparison between the vanilla Transformer and our model on the interaction style between tokens and how to deal with the uncertainty. Both models employ the label smoothed cross entropy to properly raise the uncertainty (↑) of determining a single token across the vocabulary. In addition, we **explicitly** reduce the uncertainty (↓) in the dimension of token-token interactions within a certain context to address the predictive uncertainty problem (Xiao and Wang, 2021). Definitions of some terms can be found in the Appendix.

can be reduced by feeding more data or knowledge to the model. Researchers capture and quantify uncertainties to better interpret models and enhance the representation.

Recently, almost all research fields of artificial intelligence have been deeply influenced by the Transformer (Vaswani et al., 2017). State-of-the-art neural machine translation (NMT) models are mostly built upon Transformers (Ott et al., 2018b; Dehghani et al., 2018; So et al., 2019; Zhou et al., 2020a; Liu et al., 2020). However, Transformer models also inevitably suffer from the uncertainty problem (Ott et al., 2018a; Wei et al., 2020; Xiao and Wang, 2021; Shelmanov et al., 2021). Xiao and Wang (2021) and Wei et al. (2020) handle with such problem outside of the model<sup>2</sup>. Namely, feeding more unseen samples or augmented data to the model to reduce the model uncertainty. By contrast, we address the issue inside the model. We enhance

<sup>2</sup>Note that, the word 'uncertainty' is somewhat heavily reused in the literature. For instance, Xiao and Wang (2021) incorporated uncertainty into the decoding process to reduce the hallucination. In practice, the introduced uncertainty enables the model to see otherwise unseen cases to reduce the model uncertainty in a certain context. Wei et al. (2020) employed the similar presentation. It should be appropriately distinguished from the data uncertainty and the model uncertainty in the literature (Kochkina and Liakata, 2020).

the model representation by introducing additional knowledge, namely feeding the model more relationships concerning token-token interactions in terms of nonlinear mutual dependencies.

In this paper, we aim to explicitly capture the nonlinear mutual dependencies among tokens during the attention calculation (self-attention and encoder-decoder attention in decoder) and reduce the uncertainty residing in the token-token interactions as shown in Table 1. In particular, we employ mutual information to measure the nonlinear mutual dependencies between pairs of tokens regarding the token-token interactions. Mutual information is a good measure of nonlinear relationships between random variables. To avoid the intractable feature of problems by using mutual information, we resort to InfoNCE for mutual information estimation (Logeswaran and Lee, 2018; van den Oord et al., 2019; Gutmann and Hyvärinen, 2012). InfoNCE is a mature framework for unsupervised contrastive learning. It has the theoretical and practical guarantee that a reliable lower bound can be obtained by maximizing it.

Therefore, we can explicitly obtain nonlinear mutual dependencies by regularizing the pre-trained Transformer models with maximizing mutual information. We dub the regularization of the token-token interactions in attention calculation *capturing the nonlinear mutual dependencies*. These dependencies are heavily overlooked in the vanilla Transformer, which can be employed as the additional knowledge fed to the model and reduce the model uncertainty. Experiments on WMT’14 En→De and WMT’14 En→Fr present that the performance of our model has achieved competitive results over the strong baselines and other counterparts. By contrast, to reach the same performance, contrast models either consume extra training corpus or more trainable parameters.

Contributions and highlights are as follows:

- The proposed idea is simple and makes little change to the model. It can potentially generalize to other pre-trained models leveraging self-attention.
- We explicitly capture nonlinear mutual dependencies between pairs of tokens in attentions of the decoder to reduce the model uncertainty.
- We adopt an unsupervised contrastive learning framework to estimate the mutual information,

which serves in the NMT problem.

- We present a detailed analysis of the variants of the model uncertainty before and after enhancing the mutual dependencies.

## 2 Preliminary

### 2.1 Mutual Information

Mutual information in discrete distributions is generally described as Equation 1:

$$\begin{aligned} I(X; Y) &= D_{\text{KL}}(p(X, Y) \| p(X)p(Y)) \\ &= \sum_{y \in Y} \sum_{x \in X} p(x, y) \log \left( \frac{p(x, y)}{p(x)p(y)} \right) \\ &= \mathbb{E}_{p(x, y)} \left[ \log \frac{p(x, y)}{p(x)p(y)} \right], \end{aligned} \quad (1)$$

where,  $X, Y$  denote two random variables.  $x, y$  indicate concrete samples in  $X$  and  $Y$ .  $p(\cdot)$  and  $p(\cdot, \cdot)$  represent marginal probability and joint probability respectively.  $D_{\text{KL}}$  is the Kullback–Leibler divergence (also known as the *relative entropy*) (Kullback and Leibler, 1951).

### 2.2 Contrastive Learning

Following Kong et al. (2019), we employ InfoNCE to estimate the mutual information under the contrastive learning framework. InfoNCE maximizes the mutual information to obtain a lower bound, which in practice is a good estimation of mutual information:

$$\begin{aligned} I(X, Y) &\geq \\ &\mathbb{E}_{p(X, Y)} \left[ f_{\theta}(x, y) - \mathbb{E}_{q(\tilde{Y})} \left[ \log \sum_{\tilde{y} \in \tilde{Y}} \exp f_{\theta}(x, \tilde{y}) \right] \right] \\ &+ \log |\tilde{Y}|, \end{aligned} \quad (2)$$

where,  $x$  is the positive sample token of the source sentence and  $y$  is the positive sample token of the target sentence.  $f_{\theta}$  is a measure of relevance between  $x$  and  $y$ . Usually, a similarity score function is adopted.  $\tilde{Y}$  is the negative sample set of  $y$ , note that it contains the positive sample.  $q(\cdot)$  is a distribution proposal function offering the specific rule to build the negative sample set.  $\tilde{y}$  is a random sample from the negative sample set.

The following part of Equation 2 is the crucial component when we incorporate the contrastive learning framework into the NMT problem:

$$\mathbb{E}_{p(X, Y)} \left[ f_{\theta}(x, y) - \log \sum_{\tilde{y} \in \tilde{Y}} \exp f_{\theta}(x, \tilde{y}) \right]. \quad (3)$$

### 3 Methodology

#### 3.1 Motivation to Reduce the Model Uncertainty

As mentioned in Ott et al. (2018a), a well-trained model still spreads too much probability mass across sequences. In other words, model distribution is too spread in hypothesis spaces in that it has to cater to the uncertainty brought by the data distribution. Also, as stated in Xiao and Wang (2021), unsuitable tokens attaining considerable probability mass attribute to the uncertainty of the token prediction. Moreover, Wang et al. (2019); Zhou et al. (2020b) present that lower model uncertainty indicates a better fitting of the data distribution. Therefore, in a certain context, the model uncertainty should be reasonably and appropriately reduced.

The widely adopted training paradigm is token-level teacher-forcing in NMT, which notoriously leads to the discrepancy between training and inference, namely, the exposure bias problem (Xie et al., 2016; Ranzato et al., 2016; Norouzi et al., 2016). Exposure bias partially accounts for the model uncertainty. During inference, model distribution dominates the decoding process. However, high model uncertainty directly indicates unsatisfactory fitting of the data distribution (Zhou et al., 2020b; Xiao and Wang, 2019). Canonical autoregressive generation can be formulated as Equation 4:

$$p(Y | X; \theta) = \prod_{t=1}^{N+1} p(y_t | y_{<t}, x_{1:M}; \theta), \quad (4)$$

where,  $\theta$  denotes the parameters modeling the language model.  $M$  is the length of the source sentence and  $N$  is the length of the target sentence.

At each time step, clues on the next token are all from previously generated tokens. In other words, it depends on *how much uncertainty on the next token can be reduced by knowing partially generated prefix tokens*. Vanilla Transformer implicitly reduces the uncertainty of token-token interactions during decoding. By contrast, we aim to explicitly reduce the uncertainty of the token-token interactions during the next token generation.

#### 3.2 Contrastive Learning Framework Construction in NMT

**Methods to Build the Training Samples:** Contrastive learning needs an effective and efficient relevance measure of two tokens. Specifically, a

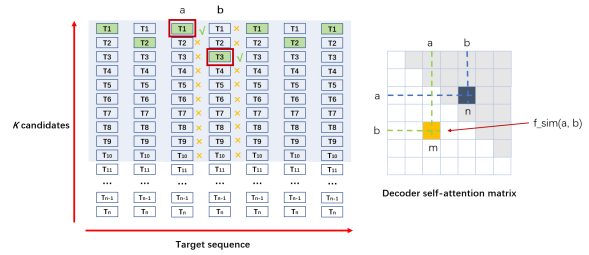


Figure 1: Graphical illustration of how to calculate  $f_{\theta}(a, b)$ .  $a$  and  $b$  denote two positions (tokens) in target sentence. In this context,  $T$  is an abbreviation for "Top", which should be distinguished from the notation of "the number of forward passes". Suppose  $T_1$  and  $T_3$  are ground-truth targets of position  $a$  and  $b$  respectively. There are two critical components composing  $f_{\theta}(a, b)$ , namely  $f_{sim}(a, b)$  and  $logit(b)$  for the pair of  $a$  and positive  $b$  while  $f_{sim}(a, b)$  and  $logit(\tilde{b})$  for the pair of  $a$  and negative sample  $\tilde{b}$  from top  $k$  candidates. The value of  $f_{sim}(a, b)$  can be directly fetched from the self-attention matrix. In the left subfigure, negative samples are from the top  $k$  candidates in position  $b$  marked by 'x' or marked by '✓', which offer  $logit(\cdot)$ . Causal self-attention matrix is demonstrated in the right sub-figure. Due to the property of symmetry, there are two  $f_{sim}(a, b)$  scores of the same value. However, position  $m$  is taken into account rather than position  $n$  in view of the causal relationship.

clear distinction should be presented between the similarity score of a positive sample  $a$  and a positive sample  $b$  and the similarity score of a positive sample  $a$  and a negative sample  $\tilde{b}$ . However, the cosine-based similarity measure solely cannot properly reflect the subtle difference in this context<sup>3</sup>. Therefore, we elaborately design a simple but effective method as Equation 5 and Equation 6:

$$f_{\theta}(x, y) = f_{sim}(x, y) + f_{logit}(y), \quad (5)$$

where,  $f_{sim}(x, y)$  is the cosine similarity score between  $x$  and  $y$  as usual.  $f_{logit}(y)$  is the logit (score before *softmax*) by the most confident prediction of  $y$  (during inference) or the logit corresponding to the ground-truth token of  $y$  (during training).

$$f_{\theta}(x, \tilde{y}) = f_{sim}(x, y) + f_{logit}(\tilde{y}), \quad (6)$$

<sup>3</sup>The vanilla cosine similarity does not elaborately distinguish the positive samples and the negative samples in this context. No matter the positives or negatives, it calculates a score. The score can be very close to each other due to the candidates from top ranking. For NMT problems under contrastive learning, we need to be deliberate in distinguishing them. Therefore, we add an explicit factor to the original cosine similarity to enhance its representation.

Model	BLEU	
	En→De	En→Fr
GNMT+RL Wu et al. (2016)	25.20	40.50
ConvS2S Gehring et al. (2017)	25.16	40.46
Transformer (base) Vaswani et al. (2017)	27.30	38.10
Transformer (big) Vaswani et al. (2017)	28.40	41.80
Evolved Transformer (big) So et al. (2019)	29.80 / 29.20	41.30
Transformer (ADMIN init) Liu et al. (2020) <sup>†</sup>	30.10 / 29.50	43.80 / 41.80
Uncertainty-Aware SANMT Wei et al. (2020)	30.29	42.92
Baseline (WMT only) Ott et al. (2018b)	29.30 / 28.60	43.20 / 41.40
Baseline (WMT+Paracrawl) Ott et al. (2018b)	29.80 / 29.30	42.10 / 40.90
Baseline (Reproduced) <sup>††</sup>	29.75 / 29.30	43.16 / 41.06
Baseline + finetuning (Contrast group) <sup>‡</sup>	29.89 / 29.40	43.17 / 41.06
Ours (Baseline+{ $L_{3,4,5}$ +DS+ED})	30.45**/29.80**	43.67*/41.51*

<sup>†</sup> The model has approx. 40M more parameters than ours.

<sup>††</sup> Our reproduced results are from the provided pre-trained checkpoints.

<sup>‡</sup> This is for a fair comparison. Results by directly finetuning fail to pass the significance tests.

Table 2: Performance comparison between different models on WMT’14 dataset. Our results are based on the reproduced results. Default values are case-sensitive *tokenized* BLEU scores and otherwise a pair of (case-sensitive *tokenized* BLEU) / (*detok. sacreBLEU*). BLEU scores are based on newstest2014 for WMT’14 English-German (En→De) and WMT’14 English-French (En→Fr). Checkpoint averaging is not used in our results. For WMT’14 En→De, we use the general configuration of  $L_{3,4,5}$ +DS+ED and  $k = 40$ . For WMT’14 En→Fr, we use the general configuration of  $L_{3,4,5}$ +DS+ED and  $k = 50$ .  $L_{3,4,5}$  indicates regularization on the layer 3,4,5 of the decoder. The definitions and usage of DS and ED can be found in Equation 8. ‘\*/\*\*’: significantly better than the baselines ( $p < 0.05$  /  $p < 0.01$ ) tested by bootstrap resampling. Note that, our results also significantly outperform the contrast groups ( $p < 0.05$ ).

where, the first part of the right-hand side is exactly the same with Equation 5. Difference between Equation 5 and Equation 6 relies on  $f_{logit}(\cdot)$ . Figure 1 depicts how to calculate the concrete value of  $f_{\theta}(a, b)$ .

Due to the steady state of the pre-trained NMT model, the component  $f_{logit}$  can take up most of the constituent that well distinguishes a legal pair of tokens with contrastive pairs. Moreover, this divergence can be further amplified due to the monotonicity of *softmax* operation. This is a key point our idea leverages to distinguish positive sample pairs from contrastive sample pairs.

**Leveraging the Pre-trained Self-attention Logits:** To fetch  $f_{sim}(x, y)$  from multi-head attention, we need a rational strategy. According to Michel et al. (2019); Voita et al. (2019); Rogers et al. (2020), it is non-trivial to partition these heads into groups. Therefore, we take as similarity scores the average of all heads as follows<sup>4</sup>:

$$F_{sim}(X, Y) = \text{Average}(\text{head}_1, \dots, \text{head}_h), \quad (7)$$

<sup>4</sup>We employed other methods to do such work, say MAX operation. However, the average operation meets our expectation.

where,  $X$  and  $Y$  are a set of tokens. Average is the average operation on similarity scores over all attention heads.  $\text{head}_*$  is a collection of similarity scores from attention heads.  $h$  is the number of attention heads.  $F_{sim}(X, Y)$  contains all pairs of similarity scores between tokens and other tokens to be attended. The value of  $f_{sim}(x, y)$  can be indexed by  $(x, y)$ .

**Combination objective:** The overall objective consists of the label smoothed cross entropy and another two custom objectives based on mutual information maximization constraints as follows:

$$\begin{aligned} \text{loss} &= (1 - \alpha - \beta) \times \text{lce\_loss} \\ &+ \alpha \times ED \\ &+ \beta \times DS, \end{aligned} \quad (8)$$

where, *lce\_loss* indicates the label smoothed cross entropy loss, *ED* represents the regularization on encoder-decoder attention and *DS* denotes the regularization on decoder self-attention. Both of them are defined and estimated as Equation 2.  $\alpha$  and  $\beta$  are hyperparameters to balance the label smoothed cross entropy loss and two custom losses.

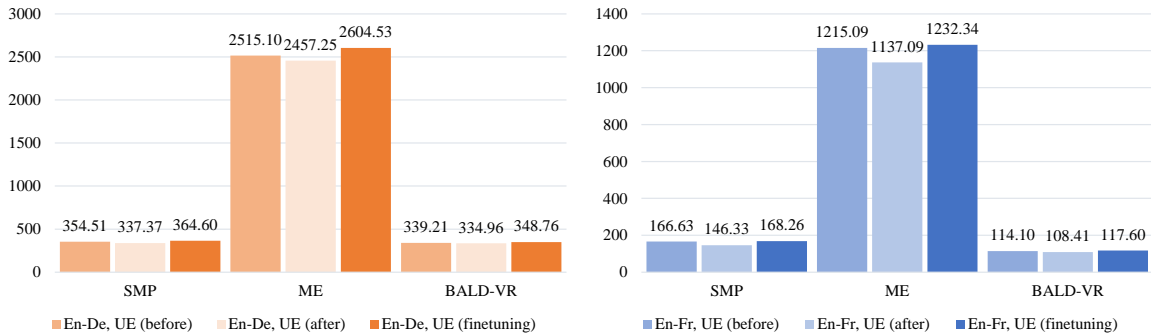


Figure 2: Variation of the model uncertainty before regularization and after regularization. The vertical axis is the model uncertainty. We employ Monte Carlo Dropout on all layers. We adopt three Uncertainty Estimation (UE) methods, namely, sampled maximum probability (SMP), mean entropy (ME) and BALD-VR to investigate the variations. The number of forward passes  $T$  is 10. The results are not normalized over the number of tokens. We add a control group for a fair comparison. We can infer that our method (histogram in the middle) reliably reduces the model uncertainty after regularization. However, directly finetuning the baselines introduces more uncertainty (histogram in the right).

## 4 Experiments

In this section, we describe the details of our experiments. We evaluate our model on WMT’14 En→De and WMT’14 En→Fr datasets. Moreover, we conduct ablation studies to assess the effectiveness of different objectives and hyperparameters setup.

### 4.1 Experimental Setup

We implement our model based on the official Fairseq toolkit implemented by PyTorch<sup>5</sup> (Ott et al., 2019) and report statistical significance tests by using compare-mt (Neubig et al., 2019)<sup>6</sup> and sacreBLEU<sup>7</sup>.

**Dataset and Metric** We train our model on WMT’14 En→De (4.5M)<sup>8</sup> and WMT’14 En→Fr (36M). For WMT’14 En→De, we validate our model on newstest13 and test on newstest2014. Following Ott et al. (2018b), we use byte pair encoding (BPE) (Sennrich et al., 2016) to prepare the joint vocabulary of 32K symbols. For WMT’14 En→Fr, we validate our model on newstest12+13 and test on newstest14. The joint vocabulary is 40K. We employ two BLEU metrics to evaluate our performance, namely, case-sensitive *tokenized* BLEU and *detokenized* sacreBLEU. We report BLEU scores with a beam size of 4 and a length penalty of 0.6.

<sup>5</sup><https://github.com/pytorch/fairseq>

<sup>6</sup><https://github.com/neulab/compare-mt>

<sup>7</sup><https://github.com/mjpost/sacreBLEU>

<sup>8</sup>To be consistent with the baseline and other counterparts, we use WMT’16 En→De to train our model and report results on the WMT’14 test set.

**Model and Hyperparameters** Our model leverages the pre-trained baseline model, which is an extension of the Transformer big model ( $d_{model} = d_{hidden} = 1024$ ,  $n_{layer} = 6$ ,  $n_{head} = 16$ ) (Vaswani et al., 2017). We adopt Adam (Kingma and Ba, 2015) to optimize our model by setting  $\beta_1 = 0.90$ ,  $\beta_2 = 0.98$  and  $\epsilon = 1e-08$ . We finetune our model from a pre-trained checkpoint with the learning rate  $3e-04$  for En→De and  $5e-04$  for En→Fr. Our criterion to configure ‘ntokens’ and ‘update-freq’ is that, neither hitting the OOM nor the threshold of the loss scale. ‘ntokens’ is 10240 for En→De and 9216 for En→Fr. ‘update-freq’ is 1 for En→De and 4 for En→Fr. The maximum epoch for En→De is 20 and 10 for En→Fr. Embeddings are shared in all positions. We tune hyperparameters on the validation set.

All experiments are conducted on a machine with 8 NVIDIA TITAN RTX GPU and a memory-efficient version of FP16 half-precision training. The proposed method has a relatively low computational overhead, taking roughly 6-7 hours for the WMT’14 En→De dataset. For the WMT’14 En→Fr dataset, it takes about two days.

### 4.2 Main Results

Table 2 demonstrates the performance comparison of our model and the baseline models along with other SOTA models on the WMT’14 dataset. We utilize a general setup of  $L_{3,4,5}$ +DS+ED to conduct the experiments. To facilitate comparison with the results of different studies, we depict both the case-sensitive *tokenized* BLEU and *detokenized*



Figure 3: Comparison between the probability mass distribution across the token vocab regarding different models (before regularization, after regularization and the contrast group). The vertical axis is the percentage of probability mass. The horizontal axis is the index of the vocab. The right figure enhances the contrast of the percentage of each of the three models to present a more intuitive visual. The experiments are conducted on the WMT’14 En→De dataset. A subset of the test set is randomly selected and employed to report the results. From the figure, it can be seen that the regularized model has a reasonable distribution of probability mass, which makes sense and is as anticipated. The contrast group is obtained by directly finetuning the pre-trained checkpoint to the same steps. However, the probability mass of the contrast group becomes inflated. From Figure 2, the contrast group introduces more uncertainty. As aforementioned, unsuitable tokens attaining considerable probability mass account for the uncertainty of the token prediction. By contrast, after regularization, our model has lower model uncertainty, and its probability mass approaches to shrink, which indicates the probability mass is properly balanced over different tokens.

SacreBLEU (Post, 2018)<sup>9</sup>. Moreover, to make a fair comparison, we also directly finetune the pre-trained checkpoints to the same steps and employ them as the contrast groups.

As shown in Table 2, it can be seen that our model achieves a compelling improvement over the strong baselines and other competitive SOTA models. Besides, our model significantly outperforms both the baseline and the contrast groups. However, the contrast group fails to pass the significance test. Therefore, we can infer that the proposed regularization method has a positive effect on the performance of the model. And our hypothesis of reducing model uncertainty by enhancing nonlinear mutual dependencies as additional knowledge is partially verified by model performance improvement. To further support our view that the performance improvement is related to the model uncertainty and dissect the relationship between the model uncertainty and the probability mass distribution across the vocab, we present more analysis in the following sections.

Since our method does minute change to the baseline models, the improvements are reasonable and justified. Additional contrast groups make our results even more convincing and credible. Moreover, it is easy to incorporate our approach to ex-

<sup>9</sup>SacreBLEU hash: BLEU+case.mixed+lang.en-de+ num-refs.1+smooth.exp+test.wmt14/full+tok.13a+version.1.4.14

isting models leveraging Transformer models. In practice, our method avoids the requirements of additional considerations for actual deployment.

### 4.3 Analysis

**Variation of Model Uncertainty:** We employ a combination of BALD (Bayesian Active Learning Disagreement) (Houlsby et al., 2011; Hazra et al., 2021) and Variation Ratio (Kochkina and Liakata, 2020) to conceptually form a new metric BALD-VR. Along with BALD-VR, we also use Mean Entropy (Kochkina and Liakata, 2020) and Sampled Maximum Probability (Shelmanov et al., 2021) to evaluate the model uncertainty, results are shown in Figure 2. From Figure 2, we can infer that the proposed method reduces the model uncertainty to some extent, which verifies our hypothesis. By contrast, the contrast group introduces more uncertainty to the model. More details are depicted in the appendix.

**Variation of the Probability Mass** As aforementioned in Section 3.1, high model uncertainty is potentially related to unsuitable probability mass distribution. We have presented that our model reduces the uncertainty and achieves better performance. However, we should unravel the relationship between the model uncertainty and the probability mass variation we assumed. To explore

310  
311  
312  
313  
314  
315  
316  
317  
318  
319  
320  
321  
322  
323  
324  
325  
326  
327  
328  
329  
330  
331  
332  
333  
334  
335  
336

337  
338  
339  
340  
341  
342  
343  
344  
345  
346  
347  
348  
349  
350  
351  
352  
353  
354  
355  
356  
357  
358  
359  
360  
361  
362  
363

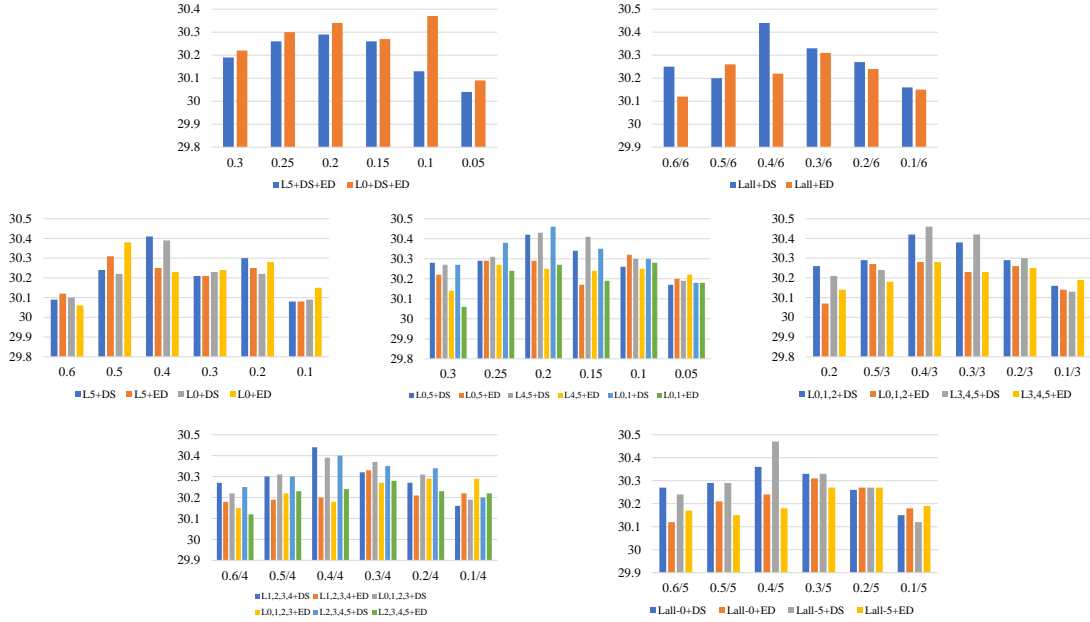


Figure 4: Ablation studies on the layer-level performance. The vertical axis is the BLEU value and the horizontal axis is the value of  $\alpha$  and  $\beta$ .  $L_*$  denotes certain layers. To simplify the experiments, we employ the same value of  $\alpha$  and  $\beta$ . We try to cover those representative cases and leave the rest for future work. Experiments are conducted on WMT’14 En→De. To reduce the overheads of training, we ignore the influence of  $k$  and set  $k = 10$  in these experiments. The definitions of DS and ED can be found in Equation 8. From these results, we can infer that ‘DS’ has a slight better performance compared with ‘ED’. Employing either ‘DS’ or ‘ED’ on all layers of the decoder is somewhat over-constraint. In a certain range, appropriately adding regularization can be effective in improving performance. Detailed results are presented in the Appendix.

the variation of model probability mass, we further analyze the probability mass distribution across token vocab dimensions with different models on the same test data. Figure 3 shows the comparison of probability mass over the three models. It can be seen that our model softens the distribution of probability mass and shrinks the probability mass of several tokens. By contrast, the probability mass distribution of the contrast group is further bloated, and within a certain range, the allocated probability mass increases. The experimental results are consistent in our model and the contrast group, including the model before regularization that the high uncertainty model has an inflated probability mass distribution, while the low uncertainty model has a relatively shrinking and more reasonable probability mass distribution.

**Correlation with the Label Smoothed Cross Entropy:** There is no conflict between the widely adopted label smoothed cross entropy (raising uncertainty) and the proposed idea (reducing uncertainty) in that they perform in the different dimensions. For clarity, label smoothing loosens a one-hot label to a soft alternative, which occurs from

the viewpoint of a single token across the vocabulary. It aims to penalize the over-confidence of the model, namely raising the model uncertainty towards a single token decision. While our approach reduces the uncertainty existing in the interactions between token and token in a certain context. It occurs from the perspective of token-token interactions, especially when a certain context is held during decoding. By contrast, our model pays attention to the inevitably introduced uncertainty that takes up non-negligible probability mass (Ott et al., 2018a). Therefore, the proposed idea is a companion to the label smoothed cross entropy rather than a replacement or alternative.

#### 4.4 Ablation Study

**Contribution of Different Objectives:** We employ two hyperparameters  $\alpha$  and  $\beta$  to balance different losses as shown in Equation 8. We validate the effectiveness of the proposed mutual information constraints by setting the hyperparameter  $1 - \alpha - \beta$  from 0.4 to 0.9. When it comes to the case of multiple layers,  $\alpha$  and  $\beta$  are equally divided by the number of layers. Results are depicted in Figure 4. From Figure 4, it is intuitive to infer that both cus-

k	1	2	3	4	5	10	20	30	40	50	100	200
BLEU	27.52	27.63	27.77	27.79	27.86	27.79	27.89	27.85	27.92	27.89	27.91	-

Table 3: The impact of different choices of  $k$  (regarding the capacity of a negative sample set) on performance. The experiment is conducted on the WMT’14 En→De valid set. A combination of two regularizations (ED+DS) is adopted. Here, the metric ’BLEU’ indicates case-sensitive *tokenized* BLEU. In the case of  $k = 200$ , the model hits the OOM under the same setup of other configurations. We use  $k = 40$  to report the final result of WMT’14 En→De. Similarly, we use  $k = 50$  to report the final result of WMT’14 En→Fr.

tom objectives have a positive impact on the model performance. ’DS’ performs slightly better than ’ED’. The boundary cases are considered as contrast groups.

**Impact of the Proposed Regularization Methods on Different Layers of the Decoder:** We conduct ablation experiments of regularization on layer-level performance in this section. Results are presented in Figure 4. From Figure 4, it can be inferred that there is no consistently positive relationship between the increase in performance and the increase in regularization on more layers. To a certain extent, appropriately adding regularization can be effective in improving performance. However, too much regularization can lead to performance degradation. We speculate that it is caused by over-regularization. Therefore, considering the performance and the overhead, we recommend that the number of regularization layers should be less than 3.

**Hyperparameter  $k$  in Contrastive Learning Framework Construction:** According to Kong et al. (2019), the larger the capacity of the negative sample set, the more accurate the framework is to estimate the lower bound of mutual information. Also, as we demonstrated in Equation 2 and Equation 3, the lower bound becomes even tighter when the number of tokens in the negative sample set is large enough. We conduct experiments with different hyperparameter  $k$  as shown in Table 3, in which we can infer that capacity of a negative sample set has a positive impact on performance in a certain range. In the case of  $k = 1$ , model performance is not far from satisfactory, which is due to the pre-trained nature of the NMT model. In other words, a pre-trained NMT model itself is a competent distribution proposal function.

## 5 Conclusion

In this paper, we propose a novel regularization method based on the maximization of mutual information. We implement our ideas under the unsu-

pervised contrastive learning framework to capture and enhance nonlinear mutual dependencies among tokens, which reduces the model uncertainty. Experiments and ablation studies demonstrate the consistent effectiveness of our approach. Besides, analysis of model uncertainty quantification again verifies our hypothesis.

**Limitation and Future Work:** To simplify the ablation studies, we employ the same weights on ’DS’ and ’ED’. Whether there will be further performance gains when taking into account regularization on different encoder layers, we will leave in the future work. Besides, our idea is based on the self-attention mechanism, which serves plenty of pre-trained language models. Nonlinear mutual dependencies may potentially have a positive influence on these models for downstream tasks. This is the first step we take to investigate how to incorporate the model uncertainty analysis into the NMT problem.

## References

- Moloud Abdar, Farhad Pourpanah, Sadiq Hussain, Dana Rezazadegan, Li Liu, Mohammad Ghavamzadeh, Paul Fieguth, Xiaochun Cao, Abbas Khosravi, U Rajendra Acharya, et al. 2020. A review of uncertainty quantification in deep learning: Techniques, applications and challenges. *arXiv preprint arXiv:2011.06225*.
- Mostafa Dehghani, Stephan Gouws, Oriol Vinyals, Jakob Uszkoreit, and Lukasz Kaiser. 2018. Universal transformers. In *International Conference on Learning Representations*.
- Yarin Gal and Zoubin Ghahramani. 2016. Dropout as a bayesian approximation: Representing model uncertainty in deep learning. In *International Conference on Machine Learning*, pages 1050–1059. PMLR.
- Jonas Gehring, Michael Auli, David Grangier, Denis Yarats, and Yann N Dauphin. 2017. Convolutional sequence to sequence learning. In *Proceedings of the 34th International Conference on Machine Learning-Volume 70*, pages 1243–1252.

494	Michael U Gutmann and Aapo Hyvärinen. 2012. Noise-	Myle Ott, Michael Auli, David Grangier, and	549
495	contrastive estimation of unnormalized statistical	Marc’Aurelio Ranzato. 2018a. Analyzing uncer-	550
496	models, with applications to natural image statistics.	tainty in neural machine translation. In <i>International</i>	551
497	<i>The journal of machine learning research</i> , 13(1):307–	<i>Conference on Machine Learning</i> , pages 3956–3965.	552
498	361.	PMLR.	553
499	Rishi Hazra, Parag Dutta, Shubham Gupta, Mo-	Myle Ott, Sergey Edunov, Alexei Baevski, Angela Fan,	554
500	hammed Abdul Qaathir, and Ambedkar Dukkipati.	Sam Gross, Nathan Ng, David Grangier, and Michael	555
501	2021. <a href="#">Active<sup>2</sup> learning: Actively reducing redundan-</a>	Auli. 2019. fairseq: A fast, extensible toolkit for	556
502	<a href="#">cies in active learning methods for sequence tagging</a>	sequence modeling. In <i>Proceedings of NAACL-HLT</i>	557
503	<a href="#">and machine translation</a> . In <i>Proceedings of the 2021</i>	<i>2019: Demonstrations</i> .	558
504	<i>Conference of the North American Chapter of the</i>	Myle Ott, Sergey Edunov, David Grangier, and Michael	559
505	<i>Association for Computational Linguistics: Human</i>	Auli. 2018b. Scaling neural machine translation. In	560
506	<i>Language Technologies</i> , pages 1982–1995, Online.	<i>Proceedings of the Third Conference on Machine</i>	561
507	Association for Computational Linguistics.	<i>Translation: Research Papers</i> , pages 1–9.	562
508	Neil Houlsby, Ferenc Huszár, Zoubin Ghahramani, and	Matt Post. 2018. A call for clarity in reporting bleu	563
509	Máté Lengyel. 2011. Bayesian active learning for	scores. In <i>Proceedings of the Third Conference on</i>	564
510	classification and preference learning. <i>arXiv preprint</i>	<i>Machine Translation: Research Papers</i> , pages 186–	565
511	<i>arXiv:1112.5745</i> .	191.	566
512	Diederik P Kingma and Jimmy Ba. 2015. Adam: A	Marc’Aurelio Ranzato, Sumit Chopra, Michael Auli,	567
513	method for stochastic optimization. In <i>International</i>	and Wojciech Zaremba. 2016. Sequence level train-	568
514	<i>Conference on Learning Representations</i> .	ing with recurrent neural networks. In <i>International</i>	569
515	Elena Kochkina and Maria Liakata. 2020. <a href="#">Estimating</a>	<i>Conference on Learning Representations</i> .	570
516	<a href="#">predictive uncertainty for rumour verification mod-</a>	Anna Rogers, Olga Kovaleva, and Anna Rumshisky.	571
517	<a href="#">els</a> . In <i>Proceedings of the 58th Annual Meeting of</i>	2020. A primer in bertology: What we know about	572
518	<i>the Association for Computational Linguistics</i> , pages	how bert works. <i>arXiv preprint arXiv:2002.12327</i> .	573
519	6964–6981, Online. Association for Computational	Rico Sennrich, Barry Haddow, and Alexandra Birch.	574
520	Linguistics.	2016. Neural machine translation of rare words with	575
521	Lingpeng Kong, Cyprien de Masson d’Autume, Lei Yu,	subword units. In <i>Proceedings of the 54th Annual</i>	576
522	Wang Ling, Zihang Dai, and Dani Yogatama. 2019.	<i>Meeting of the Association for Computational Lin-</i>	577
523	A mutual information maximization perspective of	<i>guistics (Volume 1: Long Papers)</i> , pages 1715–1725.	578
524	language representation learning. In <i>International</i>	Artem Shelmanov, Evgenii Tsymbalov, Dmitri Puzyrev,	579
525	<i>Conference on Learning Representations</i> .	Kirill Fedyanin, Alexander Panchenko, and Maxim	580
526	Solomon Kullback and Richard A Leibler. 1951. On	Panov. 2021. <a href="#">How certain is your Transformer?</a> In	581
527	information and sufficiency. <i>The annals of mathe-</i>	<i>Proceedings of the 16th Conference of the European</i>	582
528	<i>matical statistics</i> , 22(1):79–86.	<i>Chapter of the Association for Computational Lin-</i>	583
529	Xiaodong Liu, Kevin Duh, Liyuan Liu, and Jianfeng	<i>guistics: Main Volume</i> , pages 1833–1840, Online.	584
530	Gao. 2020. Very deep transformers for neural ma-	Association for Computational Linguistics.	585
531	chine translation. <i>arXiv preprint arXiv:2008.07772</i> .	David So, Quoc Le, and Chen Liang. 2019. The evolved	586
532	Lajanugen Logeswaran and Honglak Lee. 2018. An	transformer. In <i>International Conference on Machine</i>	587
533	efficient framework for learning sentence represen-	<i>Learning</i> , pages 5877–5886.	588
534	tations. In <i>International Conference on Learning</i>	Aaron van den Oord, Yazhe Li, and Oriol Vinyals. 2019.	589
535	<i>Representations</i> .	<a href="#">Representation learning with contrastive predictive</a>	590
536	Paul Michel, Omer Levy, and Graham Neubig. 2019.	<a href="#">coding</a> .	591
537	Are sixteen heads really better than one? In <i>Advances</i>	Ashish Vaswani, Noam Shazeer, Niki Parmar, Jakob	592
538	<i>in Neural Information Processing Systems</i> , pages	Uszkoreit, Llion Jones, Aidan N Gomez, Łukasz	593
539	14014–14024.	Kaiser, and Illia Polosukhin. 2017. Attention is all	594
540	Graham Neubig, Zi-Yi Dou, Junjie Hu, Paul Michel,	you need. In <i>Advances in neural information pro-</i>	595
541	Danish Pruthi, Xinyi Wang, and John Wieting. 2019.	<i>cessing systems</i> , pages 5998–6008.	596
542	<a href="#">compare-mt: A tool for holistic comparison of lan-</a>	Elena Voita, David Talbot, Fedor Moiseev, Rico Sen-	597
543	<a href="#">guage generation systems</a> .	nrich, and Ivan Titov. 2019. <a href="#">Analyzing multi-head</a>	598
544	Mohammad Norouzi, Samy Bengio, Navdeep Jaitly,	<a href="#">self-attention: Specialized heads do the heavy lift-</a>	599
545	Mike Schuster, Yonghui Wu, Dale Schuurmans, et al.	<a href="#">ing, the rest can be pruned</a> . In <i>Proceedings of the</i>	600
546	2016. Reward augmented maximum likelihood for	<i>57th Annual Meeting of the Association for Computa-</i>	601
547	neural structured prediction. In <i>Advances In Neural</i>	<i>tional Linguistics</i> , pages 5797–5808, Florence, Italy.	602
548	<i>Information Processing Systems</i> , pages 1723–1731.	Association for Computational Linguistics.	603

604 Shuo Wang, Yang Liu, Chao Wang, Huanbo Luan, and  
605 Maosong Sun. 2019. [Improving back-translation  
606 with uncertainty-based confidence estimation](#). In  
607 *Proceedings of the 2019 Conference on Empirical  
608 Methods in Natural Language Processing and the 9th  
609 International Joint Conference on Natural Language  
610 Processing (EMNLP-IJCNLP)*, pages 791–802, Hong  
611 Kong, China. Association for Computational Linguistics.  
612

613 Xiangpeng Wei, Heng Yu, Yue Hu, Rongxiang Weng,  
614 Luxi Xing, and Weihua Luo. 2020. [Uncertainty-  
615 aware semantic augmentation for neural machine  
616 translation](#). In *Proceedings of the 2020 Conference  
617 on Empirical Methods in Natural Language Process-  
618 ing (EMNLP)*, pages 2724–2735, Online. Association  
619 for Computational Linguistics.

620 Yonghui Wu, Mike Schuster, Zhifeng Chen, Quoc V Le,  
621 Mohammad Norouzi, Wolfgang Macherey, Maxim  
622 Krikun, Yuan Cao, Qin Gao, Klaus Macherey, et al.  
623 2016. Google’s neural machine translation system:  
624 Bridging the gap between human and machine trans-  
625 lation. *arXiv preprint arXiv:1609.08144*.

626 Yijun Xiao and William Yang Wang. 2019. Quantifying  
627 uncertainties in natural language processing tasks.  
628 In *Proceedings of the AAAI Conference on Artificial  
629 Intelligence*, volume 33, pages 7322–7329.

630 Yijun Xiao and William Yang Wang. 2021. [On hal-  
631 lucination and predictive uncertainty in conditional  
632 language generation](#). In *Proceedings of the 16th Con-  
633 ference of the European Chapter of the Association  
634 for Computational Linguistics: Main Volume*, pages  
635 2734–2744, Online. Association for Computational  
636 Linguistics.

637 Ziang Xie, Sida I Wang, Jiwei Li, Daniel Lévy, Aiming  
638 Nie, Dan Jurafsky, and Andrew Y Ng. 2016. Data  
639 noising as smoothing in neural network language  
640 models.

641 Long Zhou, Jiajun Zhang, and Chengqing Zong.  
642 2020a. [Improving autoregressive NMT with non-  
643 autoregressive model](#). In *Proceedings of the First  
644 Workshop on Automatic Simultaneous Translation*,  
645 pages 24–29, Seattle, Washington. Association for  
646 Computational Linguistics.

647 Yikai Zhou, Baosong Yang, Derek F. Wong, Yu Wan,  
648 and Lidia S. Chao. 2020b. [Uncertainty-aware cur-  
649 riculum learning for neural machine translation](#). In  
650 *Proceedings of the 58th Annual Meeting of the Asso-  
651 ciation for Computational Linguistics*, pages 6934–  
652 6944, Online. Association for Computational Lin-  
653 guistics.

## 654 Appendix

### 655 A Terminology

656 **Token-token interactions** We refer to ‘token-  
657 token interactions’ as the process of a token attend-  
658 ing to the other token and formulating its represen-  
659 tation by linear interpolation (vanilla Transformer)

of relative candidates. There are three types of at-  
660 tention in a Transformer model. The behavior of  
661 token-token interactions is different in each atten-  
662 tion. We concentrate on the attention mechanism  
663 in the decoder, namely the self-attention in the de-  
664 coder and the encoder-decoder attention in the de-  
665 coder. Given the causal feature of the self-attention  
666 in the decoder, we should value the masking mech-  
667 anism. The architecture of the vanilla Transformer  
668 model is shown in Figure 5. 669

**Maximizing mutual information** Mathemati-  
670 cally, mutual information is a good measure of  
671 nonlinear relationships between random variables.  
672 Mutual information quantifies the information on  
673 one token to be predicted given previous gener-  
674 ated one in the context of sequence generation. By  
675 maximizing mutual information among tokens dur-  
676 ing token-token interactions, we can capture more  
677 nonlinear mutual dependencies. We name the pro-  
678 cess of maximizing mutual information during fine-  
679 tuning regularization. We refer to ‘enhancing the  
680 nonlinear mutual dependencies’ as the process of  
681 regularization, in other words, maximizing mutual  
682 information. The nonlinear mutual dependencies  
683 we captured can be seen as additional knowledge  
684 extracted from the training corpus. Extra training  
685 corpus or knowledge is capable of reducing the  
686 model uncertainty. We propose our method to re-  
687 duce the model uncertainty in terms of feeding this  
688 knowledge from the existing training corpus. From  
689 the perspective of linguistics, the enhanced repre-  
690 sentation can reinforce token-token connections in  
691 some contexts. 692

**Enhancing nonlinear mutual dependencies** En-  
693 hancing or capturing nonlinear mutual dependen-  
694 cies is equal to maximizing mutual information  
695 among tokens or regularization on attention cal-  
696 culation in the decoder. *Why nonlinear?* Linear  
697 interpolation of representation is intrinsic in the at-  
698 tention mechanism of vanilla Transformer models.  
699 Compared with nonlinear, linear interpolation has  
700 a feature of limited expressiveness. *Why mutual  
701 information?* Mutual information captures such  
702 nonlinear relationships. What are the *dependen-*  
703 *cies?* Relationships or connections of tokens. 704

**Model uncertainty** Model uncertainty is also  
705 known as epistemic uncertainty. It describes  
706 whether the model we employ can well fit the data  
707 distribution. Model design and selection accounts  
708 for the model uncertainty. Model uncertainty can  
709

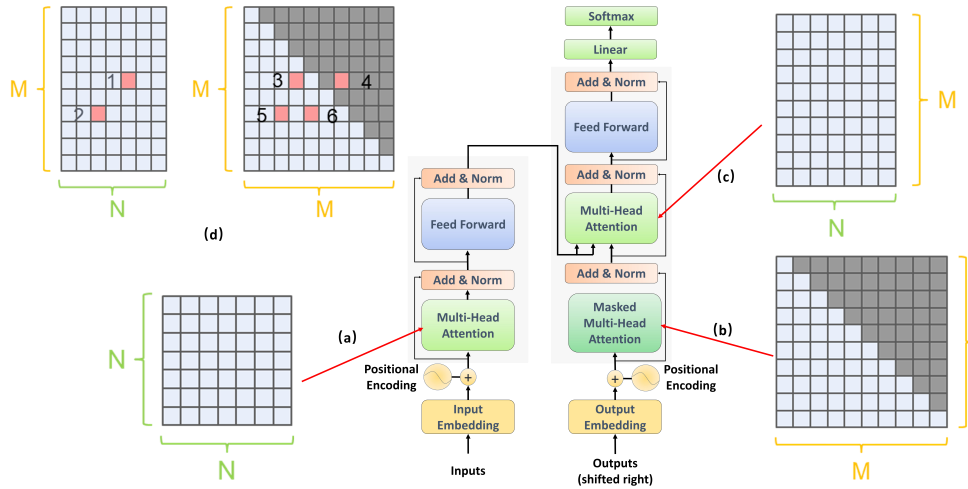


Figure 5: Transformer model and self-attentions. (a) Self-attention in the encoder. Queries, keys, and values are the same. It is a symmetric matrix. The outputs of the last layer serve as the keys and values of the encode-decoder attention in the decoder. (b) Decoder self-attention. Queries, keys, and values are the same as the outputs of the decoder step by step. It is also a square matrix. Only positions of the lower triangular region are legal. Black blocks indicate those positions masked to keep the causal property. (c) Encoder-decoder attention in the decoder. Queries are from outputs of decoder self-attention. Due to the different lengths between the source and target sentence, this is generally a non-square matrix. In (d), Mark 1 or Mark 2 indicate a target token (indexed by row number) attends to a source token (indexed by column number) in encoder-decoder attention in the decoder, respectively. It is also a convenient lookup table to fetch the cosine similarity score of pairs of tokens employed in calculating mutual information. In (d), a token can attend to Mark 3 but not Mark 4 due to its causal nature. By contrast, Mark 5 and Mark 6 can be attended by tokens indexed by the row number.

710 be reduced by feeding more data or knowledge  
 711 to the model. Both model uncertainty and data  
 712 uncertainty affect the prediction. In this work,  
 713 we concentrate on the *model* uncertainty. Follow-  
 714 ing Shelmanov et al. (2021); Zhou et al. (2020b);  
 715 Xiao and Wang (2019); Wang et al. (2019), we  
 716 employ Monte Carlo Dropout (Gal and Ghahra-  
 717 mani, 2016) to approximate Bayesian inference to  
 718 conduct the Uncertainty Estimation (UE). Specifi-  
 719 cally, we demonstrate the quantification of model  
 720 uncertainty before and after the regularization to  
 721 investigate the variation:

$$\begin{aligned}
 & UE(\theta) \\
 &= \frac{1}{N} \sum_{n=1}^N \text{Var} \left[ P \left( y^n \mid x^n, \hat{\theta}^t \right) \right]_{t=1}^T, \quad (9)
 \end{aligned}$$

723 where,  $\theta$  is the set of model parameters.  $x$  and  
 724  $y$  are training samples.  $N$  indicates the num-  
 725 ber of samples.  $T$  is the number of stochastic  
 726 passes.  $\{\hat{\theta}^1, \dots, \hat{\theta}^T\}$  are sampled parameters dur-  
 727 ing stochastic passes. To be consistent with Wang  
 728 et al. (2019), we calculate the uncertainty after the  
 729 prediction process is done in that we do not employ  
 730 the model uncertainty to improve the model predic-  
 731 tion, instead, we quantify the model uncertainty.

732 **Data uncertainty** Data uncertainty is also named  
 733 aleatoric uncertainty. For NLP problems, the se-  
 734 mantically equivalent transformation of sentences  
 735 or tokens attributes to the data uncertainty. Be-  
 736 sides, noisy data generated during the collection of  
 737 training corpus can also introduce data uncertainty.

738 **Reducing the model uncertainty** High model  
 739 uncertainty indicates the poor fitting of the data  
 740 distribution, which results in worse model perfor-  
 741 mance. Either feeding more data or additional  
 742 knowledge can reduce the model uncertainty. We  
 743 regard these nonlinear mutual dependencies ex-  
 744 tracted by regularizing the model as additional  
 745 knowledge fetched from the training corpus. Be-  
 746 sides, reducing the model uncertainty is roughly  
 747 equal to raising the model confidence of decision-  
 748 making in a certain context. Why we would like to  
 749 *reduce* the model uncertainty? And is there any cor-  
 750 relation between model uncertainty and translation  
 751 quality? There are at least two perspectives to ana-  
 752 lyze these questions. For instance, as we mentioned  
 753 in Table 1 and also in the Section "Correlation with  
 754 the Label Smoothed Cross Entropy". In some cases,  
 755 an appropriate **increase** in the model uncertainty  
 756 can generalize the model performance. A good ex-

757	ample is that the widely employed label smoothed	<b>tween the NMT problem and the mutual infor-</b>	807
758	cross entropy properly raises the uncertainty of	<b>mation.</b> We suppose that maximizing the mutual	808
759	determining a <b>single</b> token across the vocabulary.	information could be helpful in the NMT system	809
760	Because the generalization capability of the model	from the perspective of reducing the model uncer-	810
761	is enhanced, the translation quality becomes better.	tainty.	811
762	From another perspective of <b>token-token</b> interac-	To this end, on one hand, we evaluate the per-	812
763	tions, our approach <b>reduces</b> the uncertainty exist-	formance of translation in the form of the widely	813
764	ing in the interactions between token and token	employed BLEU value. On the other hand, we also	814
765	in a certain context. The model uncertainty can	verify our hypothesis by quantifying the model	815
766	be reduced by feeding more data or knowledge to	uncertainty before regularization and after regu-	816
767	the model. Therefore, we employ more knowledge	larization. Besides, given that there are relatively	817
768	in terms of nonlinear relationships to reduce the	few relevant studies in this research, we also pro-	818
769	model uncertainty. Please note that our method is	vide some abbreviated analyses of the analytical	819
770	based on enhancing the model representation of	methods.	820
771	token-token interactions, in other words, it occurs		
772	in a certain context. Intuitively, the model could	<b>C Detailed Experimental Results</b>	821
773	be more confident when making decisions in cer-	Some detailed experimental results are presented	822
774	tain contexts. This is reasonable and makes sense.	in Table 4, Table 5, Table 6, and Table 7 for further	823
775	From this point of view, an appropriate reduction	reference.	824
776	of model uncertainty can increase the quality of the		
777	translation.	<b>D Hyperparameters in MC Dropout</b>	825
		<b>Inference</b>	826
778	<b>B Motivation and Connection Between</b>	Two key factors that affect the MC dropout infer-	827
779	<b>Different Terms</b>	ence. Namely, the number of forward passes $T$ and	828
780	In this section, we further clarify our motiva-	the dropout ratio $p$ . We investigate such factors in	829
781	tion and describe some inner connections between	this section. We conduct ablation experiments and	830
782	newly introduced concepts.	demonstrate the results in Figure 6. From Figure 6,	831
783	We found in the literature that the use of uncer-	we can infer that $T = 10$ and $p = 0.3$ meet the	832
784	tainty reduction can help solve other NLP prob-	requirements.	833
785	lems. And the famous Transformer model in the		
786	NMT problem has the predictive uncertainty prob-		
787	lem. Therefore, we aim to introduce a certain		
788	approach to reduce such predictive uncertainty in		
789	Transformer. Most existing research concentrates		
790	on feeding more data to the model to reduce the		
791	model uncertainty. By contrast, we would like to		
792	enhance the model representation by introducing		
793	additional knowledge, namely feeding the model		
794	more relationships between token-token interac-		
795	tions.		
796	The interactions among two tokens in a sentence		
797	are obtained by a weighted summation in a lin-		
798	ear fashion. We would like to capture more re-		
799	lationships among tokens beyond what we know.		
800	Therefore, <b>mutual information</b> occurs to us. We		
801	employ InfoNCE to approximate the mutual infor-		
802	mation. To facilitate problem-solving, we also for-		
803	mulate the whole problem under the framework of		
804	contrastive learning. We can maximize the mutual		
805	information by InfoNCE to obtain a lower bound.		
806	So far, we have established <b>the relationship be-</b>		

	Models <sup>†</sup>					
$1 - \alpha - \beta$	0.4	0.5	0.6	0.7	0.8	0.9
$\alpha, \beta$	0.6/2	0.5/2	0.4/2	0.3/2	0.2/2	0.1/2
$L_5$ +DS+ED	30.19/29.50	30.26/29.60	30.29/29.60	30.26/29.60	30.13/29.50	30.04/29.40
$L_0$ +DS+ED	30.22/29.50	30.30/29.60	30.34/29.60	30.27/29.60	30.37/29.80	30.09/29.50
$\alpha, \beta$	0.6	0.5	0.4	0.3	0.2	0.1
$L_5$ +DS	30.09/29.40	30.24/29.50	30.41/29.70	30.21/29.60	30.30/29.70	30.08/29.50
$L_5$ +ED	30.12/29.40	30.31/29.60	30.25/29.50	30.21/29.60	30.25/29.70	30.08/29.50
$L_0$ +DS	30.10/29.40	30.22/29.50	30.39/29.70	30.23/29.60	30.22/29.60	30.09/29.50
$L_0$ +ED	30.06/29.40	30.38/29.70	30.23/29.50	30.24/29.60	30.28/29.70	30.15/29.50
$\alpha, \beta$	0.6/2	0.5/2	0.4/2	0.3/2	0.2/2	0.1/2
$L_{0,5}$ +DS	30.28/29.60	30.29/29.60	30.42/29.70	30.34/29.70	30.26/29.60	30.17/29.60
$L_{0,5}$ +ED	30.22/29.50	30.29/29.60	30.29/29.60	30.17/29.50	30.32/29.70	30.20/29.60
$L_{4,5}$ +DS	30.27/29.60	30.31/29.60	30.43/29.70	30.41/29.70	30.30/29.70	30.19/29.60
$L_{4,5}$ +ED	30.14/29.40	30.27/29.60	30.25/29.60	30.24/29.60	30.25/29.70	30.22/29.70
$L_{0,1}$ +DS	30.27/29.60	30.38/29.70	30.46/29.70	30.35/29.70	30.30/29.70	30.18/29.60
$L_{0,1}$ +ED	30.06/29.30	30.24/29.60	30.27/29.60	30.19/29.60	30.28/29.70	30.18/29.60
$\alpha, \beta$	0.6/3	0.5/3	0.4/3	0.3/3	0.2/3	0.1/3
$L_{0,1,2}$ +DS	30.26/29.60	30.29/29.60	30.42/29.70	30.38/29.70	30.29/29.70	30.16/29.60
$L_{0,1,2}$ +ED	30.07/29.40	30.27/29.60	30.28/29.60	30.23/29.60	30.26/29.70	30.14/29.60
$L_{3,4,5}$ +DS	30.21/29.50	30.24/29.50	30.46/29.70	30.42/29.70	30.30/29.70	30.13/29.60
$L_{3,4,5}$ +ED	30.14/29.50	30.18/29.50	30.28/29.60	30.23/29.60	30.25/29.70	30.19/29.60
$\alpha, \beta$	0.6/4	0.5/4	0.4/4	0.3/4	0.2/4	0.1/4
$L_{1,2,3,4}$ +DS	30.27/29.60	30.30/29.60	30.44/29.70	30.32/29.70	30.27/29.70	30.16/29.60
$L_{1,2,3,4}$ +ED	30.18/29.50	30.19/29.60	30.20/29.50	30.33/29.70	30.21/29.60	30.22/29.70
$L_{0,1,2,3}$ +DS	30.22/29.50	30.31/29.60	30.39/29.70	30.37/29.70	30.31/29.70	30.19/29.60
$L_{0,1,2,3}$ +ED	30.15/29.40	30.22/29.50	30.18/29.50	30.27/29.60	30.29/29.70	30.29/29.60
$L_{2,3,4,5}$ +DS	30.25/29.50	30.30/29.60	30.40/29.70	30.35/29.70	30.34/29.70	30.20/29.60
$L_{2,3,4,5}$ +ED	30.12/29.40	30.23/29.60	30.24/29.60	30.28/29.70	30.23/29.70	30.22/29.60
$\alpha, \beta$	0.6/5	0.5/5	0.4/5	0.3/5	0.2/5	0.1/5
$L_{all-0}$ +DS	30.27/29.60	30.29/29.60	30.36/29.60	30.33/29.70	30.26/29.60	30.15/29.60
$L_{all-0}$ +ED	30.12/29.40	30.21/29.60	30.24/29.60	30.31/29.70	30.27/29.70	30.18/29.60
$L_{all-5}$ +DS	30.24/29.50	30.29/29.60	30.47/29.70	30.33/29.70	30.27/29.70	30.12/29.60
$L_{all-5}$ +ED	30.17/29.50	30.15/29.50	30.18/29.50	30.27/29.60	30.27/29.70	30.19/29.60
$\alpha, \beta$	0.6/6	0.5/6	0.4/6	0.3/6	0.2/6	0.1/6
$L_{all}$ +DS	30.25/29.50	30.20/29.60	30.44/29.70	30.33/29.70	30.27/29.60	30.16/29.60
$L_{all}$ +ED	30.12/29.40	30.26/29.60	30.22/29.50	30.31/29.70	30.24/29.70	30.15/29.60

<sup>†</sup> We tune the parameters on the validation set, and report these results on the test set. Values in this table may be susceptible to different setups that we did not thoroughly explore. However, we do not aim to provide the best situations of all cases, instead, we offer analysis of possible trends. We ignore the influence of  $k$  and set  $k = 10$  in these experiments.

Table 4: Ablation studies on the layer-level performance. 'DS' indicates the proposed regularization approach applied on the decoder self-attention. 'ED' means the proposed regularization approach applied on the encoder-decoder attention in the decoder. To simplify the experiments, we adopt the same value of  $\alpha$  and  $\beta$  to balance 'DS' and 'ED'. For instance, if the weight on the label smoothed cross entropy is  $w$ , then  $\alpha, \beta = (1 - w)/2$ , when 'DS' and 'ED' are applied on a single layer of the decoder. Similarly,  $\alpha, \beta = (1 - w)/6$ , when 'DS' or 'ED' are applied on all layers of the decoder, and so on. Different contributions of 'DS' or 'ED' in the combination fashion of 'DS+ED', we leave them in the future work.  $L_0$  means the first layer in the decoder.  $L_5$  means the last layer.  $L_{0,5}$  means the first layer and the last layer.  $L_{4,5}$  means the last two layers.  $L_{0,1}$  means the first two layers.  $L_{0,1,2}$  means the first three layers.  $L_{3,4,5}$  means the last three layers.  $L_{all-0}$  means all layers except the first layer.  $L_{all-5}$  means all layers except the last layer. We average the last 5 checkpoints to report these results. Experiments are conducted on WMT'14 En→De. From these results, we can infer that 'DS' has slight better performance compared with 'ED'. Employing either 'DS' or 'ED' on all layers of the decoder is somewhat over-constraint. In a certain range, appropriately adding regularization can be effective in improving performance.

Dropout Type	Model Acquisition	En→De		En→Fr	
		UE (before)	UE (after)	UE (before)	UE (after)
MC-all	Sampled max. probability	354.5077	337.3681	166.6318	146.3338
MC-all	Mean entropy	2515.1008	2457.2503	1215.0922	1137.0944
MC-all	BALD-VR	339.2128	334.9575	114.1011	108.4149

Table 5: Variation of the model uncertainty before regularization and after regularization. ‘MC-all’ means ‘Monte Carlo Dropout’ employed on all layers. We employ three Uncertainty Estimation (UE) methods, namely, Sampled max. probability, Mean Entropy and BALD-VR to investigate the variations. The number of forward passes  $T$  is 10. The results are not normalized over the number of tokens.

Num. of $T$	1	2	3	4	5	6
SMP	338.0088 / 319.5488	347.5487 / 329.9464	350.2366 / 333.0439	351.9552 / 334.9495	353.7504 / 335.7504	353.4781 / 336.2595
ME	2403.5835 / 2341.8491	2460.3462 / 2400.5967	2479.6318 / 2421.1494	2492.6663 / 2435.1404	2500.8201 / 2441.8916	2504.8918 / 2445.9519
BALD-VR	0 / 0 <sup>†</sup>	154.9255 / 150.7553	214.0106 / 210.4574	251.8404 / 246.7234	275.8936 / 270.2872	294.9787 / 288.6808
Num. of $T$	7	8	9	10	20 <sup>‡</sup>	30 <sup>‡</sup>
SMP	353.6949 / 336.5727	353.9379 / 336.8132	354.3253 / 337.1445	354.5077 / 337.3681	176.3070 / 168.1396	87.0544 / 83.3469
ME	2507.3079 / 2449.6633	2509.6550 / 2451.1414	2512.8601 / 2454.7310	2515.1008 / 2457.2503	1249.8004 / 1224.1233	615.8340 / 605.8625
BALD-VR	307.9149 / 303.4787	321.2128 / 315.9893	331.2021 / 326.0425	339.2128 / 334.9575	193.9734 / 192.5053	101.8218 / 101.2766

<sup>†</sup> Zero values are due to the calculation of variance towards a single value.

<sup>‡</sup> In the case of  $T = 20$  and  $T = 30$ , results seem to be disproportionate to other cases. This is due to the setup of batch size during inference in order to avoid OOM.

Table 6: The impact of the number of forward passes  $T$  on MC dropout inference. We show the variations of the three metrics. ‘SMP’ for ‘sampled maximum probability’; ‘ME’ for ‘mean entropy’; ‘BALD-VR’ for a combination of ‘Bayesian Active Learning by Disagreement’ and ‘variation ratio’. The values presented here are UE (before) / UE (after). Experiments are conducted on WMT’14 En→De. Dropout ratio  $p$  is the default value 0.3. We can infer that as the value  $T$  increases, the gap between two UEs tends to decrease. However, UE (after) is consistently smaller than UE (before). Considering the practical situation and following the common literature, we choose  $T = 10$  throughout the experiments.

dropout ratio $p$	0.1	0.2	0.3 <sup>†</sup>	0.4	0.5
SMP	302.3890 / 286.0438	323.7969 / 306.6345	354.5077 / 337.3681	403.9660 / 388.3170	<del>495.5341 / 485.3623</del>
ME	2057.5542 / 1990.6696	2240.8325 / 2173.9890	2515.1008 / 2457.2503	2962.1492 / 2926.7832	<del>3779.8779 / 3796.4238</del>
BALD-VR	234.0745 / 231.3511	285.9575 / 282.3511	339.2128 / 334.9575	406.0213 / 403.2021	<del>529.4787 / 537.0319</del>
dropout ratio $p$	0.6	0.7	0.8	0.9	1.0
SMP	<del>698.8461 / 703.8344</del>	<del>890.4090 / 887.0627</del>	<del>940.6628 / 943.8118</del>	<del>955.7371 / 955.7843</del>	<del>868.1199 / 868.6059</del>
ME	<del>5537.7705 / 5691.3364</del>	<del>7761.6455 / 7963.3516</del>	<del>9321.2520 / 9468.3799</del>	<del>9783.8789 / 9785.2402</del>	<del>5698.2153 / 5684.1841</del>
BALD-VR	<del>803.1170 / 823.4362</del>	<del>954.4681 / 955.8192</del>	<del>957.7553 / 957.7553</del>	<del>957.7553 / 957.7553</del>	<del>0 / 0</del>

<sup>†</sup> There are three main types of dropout operation in the implementation of Transformer model, namely, dropout for layer output, dropout for attention weights and dropout for activation in FFN. Here, we refer ‘dropout’ to the first case. Note that, 0.3 is the default value for WMT’14 En→De model.

Table 7: The impact of the dropout ratio  $p$  on MC dropout inference. We show the variations of the three metrics. ‘SMP’ for ‘sampled maximum probability’; ‘ME’ for ‘mean entropy’; ‘BALD-VR’ for a combination of ‘Bayesian Active Learning by Disagreement’ and ‘variation ratio’. The values presented here are UE (before) / UE (after). Experiments are conducted on WMT’14 En→De. The number of forward passes  $T$  is 10. From the results above, we can infer that the appropriate value of the dropout ratio  $p$  is no more than 0.4, which is in line with our expectations. Bad cases are marked by ~~strikethrough~~.

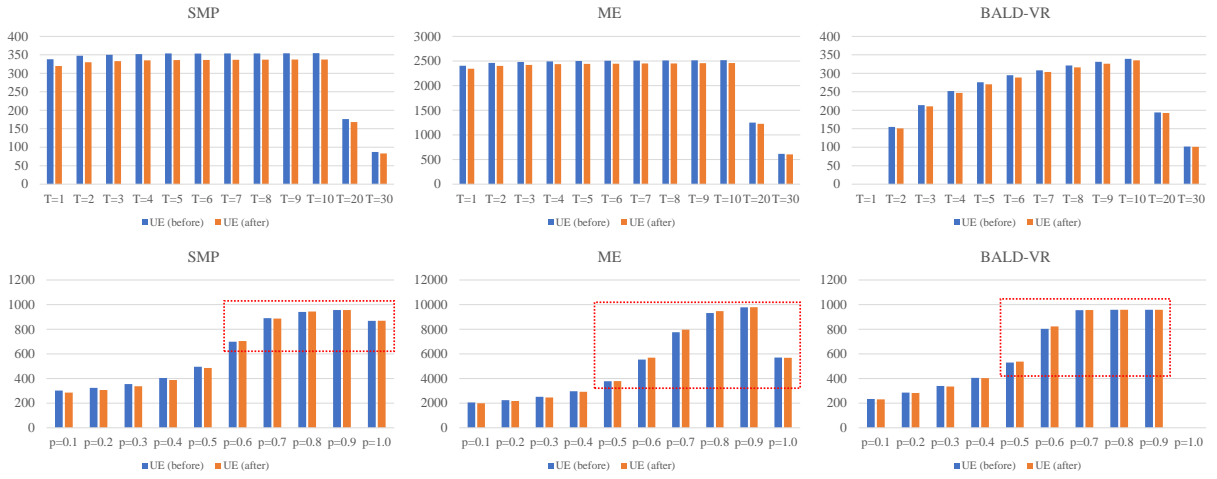


Figure 6: Experiments on the selection of hyperparameters in uncertainty estimation. The vertical axis is the unnormalized model uncertainty score and the horizontal axis is the number of forward pass  $T$  in the figures of the first row, and the dropout ratio  $p$  in the figures of the second row. Bad cases are marked by red boxes. From these ablation results, we can infer that the number of  $T$  has little impact on performance in our work. Following the general literature, we employ  $T = 10$  throughout the experiments. However, the dropout ratio  $p$  matters a lot. From the results shown above, we should use a value less than 0.4. Therefore, we adopt  $p = 0.3$  throughout the experiments.